ELSEVIER

Contents lists available at ScienceDirect

Journal of Hydrology

journal homepage: www.elsevier.com/locate/jhydrol



Research papers



Biogeochemistry of dissolved and particulate phosphorus speciation in the Maowei Sea, northern Beibu Gulf

Cheng Xu^{a,b,c}, Solomon Felix Dan^{a,1}, Bin Yang^{a,d,e,*}, Dongliang Lu^a, Zhenjun Kang^{a,e}, Haifang Huang^a, Jiaodi Zhou^a, Zhiming Ning^d

- ^a Guangxi Key Laboratory of Marine Disaster in the Beibu Gulf, Beibu Gulf University, Qinzhou 535011, China
- ^b State Key Laboratory of Estuarine and Coastal Research, East China Normal University, Shanghai 200062, China
- College of Chemistry and Bioengineering, Guilin University of Technology, Guilin 541000, China
- d Guangxi Laboratory on the Study of Coral Reefs in the South China Sea, Guangxi University, Nanning 530004, China
- e Key Laboratory of Coastal Science and Engineering, Beibu Gulf University, Qinzhou 535011, China

ARTICLE INFO

Keywords: Phosphorus Chemical speciation Biogeochemical processes Maowei Sea

ABSTRACT

Phosphorus (P) is an important biogenic element that limits algal growth, and influences primary productivity and biogeochemical cycling of other biogenic elements in freshwater and marine ecosystems. Surface water samples were collected along the salinity gradients from the western and eastern flanks of the Maowei Sea (MWS) during July 2018 for measurements of different P species, including dissolved nitrogen and silicate. Total dissolved P (TDP) dominated the total P (TP) accounting for $64.9 \pm 9.7\%$ of TP, possibly due to relatively less suspended particulate matter (<100 mg/L). Among the dissolved P species, dissolved organic P (DOP) was more abundant (DOP/TDP = $58.1 \pm 20\%$) than dissolved inorganic P (DIP). Considering the entire dataset, the average DIP concentration (1.53 \pm 0.83 μ M) was lower to medium range, while DOP was relatively higher, compared to other estuaries and coastal waters bodies worldwide. Particulate P was mainly present as particulate inorganic P (PIP), which accounted for $68.5 \pm 9.0\%$ of the total particulate P (TPP). The behavior of different P species along the salinity gradients indicated that their concentrations were dominantly influenced by riverine inputs and biogeochemical processes. Intensive mariculture activities in the MWS may have also contributed to elevated DOP compared to other coastal marine systems worldwide. Apart from similar sources of input and cycling processes, the stoichiometric relationship between DIP, dissolved inorganic N (DIN) and dissolved silicate (DSi) suggested that P is potentially limiting, while Si may co-limit primary productivity. The latitudinal distribution of different P species indicated that strong transformations existed between the particulate and dissolved P phases along the salinity gradients. The negative relationship between P partitioning coefficient [log(K_d)] and salinity, and with suspended particulate matter (log[SPM]) suggested that strong particle reactivity and probable competition between dissolved P with other anions for adsorption sites influenced the partitioning of P species in surface water. Additionally, the end-member binary model showed that \sim 1.24–1.55 μ M of DIP may have been removed through biological uptake. In summary, this study shows that the dynamic changes in the concentrations, spatial distribution, and transformation process of different P species between dissolved and particulate phases can effectively reveal the sources of P and understand the internal relationship between the biogeochemical cycling of P, stoichiometric status, and eutrophication.

1. Introduction

Phosphorus (P) is an essential bio-limiting macronutrient in the biosphere, and play crucial roles in regulating ecosystem function and primary productivity in freshwater and coastal marine systems

(Björkman and Karl, 2003; Slomp et al., 2004; Yang et al., 2018a). The lower concentration of P in many aquatic environments is partly due to the solubility of apatite (being the commonest naturally occurring mineral containing P in the Earth's crust) in freshwater, which is generally <0.4% wt (Ayers and Watson, 1991), and thus, the dissolved P

^{*} Corresponding author at: Guangxi Key Laboratory of Marine Disaster in the Beibu Gulf, Beibu Gulf University, Qinzhou 535011, China. *E-mail address:* binyang@bbgu.edu.cn (B. Yang).

¹ Cheng Xu and Solomon Felix Dan contributed equally to this study.

levels in pristine or less contaminated environments are generally < 0.5 μM. Other biogenic elements such as nitrogen (N) and silica (Si) are also essential for the ecological sustainability of an aquatic ecosystem. Therefore, the contents and distributions of N and Si in dissolved phase and their stoichiometric relationships with P may generally influence nutrient structures and behavior, with important ecological implications on primary productivity and phytoplankton species composition (Duan et al., 2016; Dan et al., 2019). In the last three decades, anthropogenic perturbations in coastal areas have increased the concentration of dissolved inorganic P (DIP) up to \sim 2-3 fold in some larger rivers worldwide (Wang et al., 2018; Cozzi et al., 2019). Comparatively, DIP concentrations in small, medium river systems and bays have become elevated (exceeding $10 \mu M$) than in the world's large rivers (van der Zee et al., 2007; Eliani-Russak et al., 2013), due to industrial and agricultural activities around small river basins that lack stringent regulations of local government, and especially in bays that have weak capacity of self-purification (Pan et al., 2020). The loading of P beyond pristine levels mostly results in eutrophication and bottom water hypoxia due to an abnormal algal production in estuarine and coastal marine environments (Lin et al., 2018). Total P (TP) has been reported as an insufficient measure to evaluate P speciation and predict its potential bioavailability in coastal waters (e.g., Dan et al., 2020a, 2020b). However, studies on different forms of P (i.e., inorganic, or organic) with their different chemical reactivity and speciation, have been proposed to understand the biogeochemical behavior and bioavailability of P not only in sediments but also in the water column. Thus, knowledge of the abundance, speciation, distributions, and transformation of P is essential for a better understanding of P behavior and ecosystem quality in coastal marine environments (Benitez-Nelson, 2000; Lin et al., 2016; Yang et al., 2016).

In natural waters, TP is mainly partitioned into dissolved inorganic P (DIP), dissolved organic P (DOP), particulate inorganic P (PIP) and particulate organic P (POP) phases (van der Zee et al., 2007; Lin et al., 2012; Karl, 2014; Lin and Guo, 2016). The PIP and POP together constitutes the total particulate P (TPP) pool, while DOP and DIP together constitutes the total dissolved P (TDP) pool. Aquatic living creatures or detrital organic matter are the major components of POP, while PIP occurs in mineral phases with complex components (Duan et al., 2016; Li et al., 2017), which includes the adsorbed P, and co-precipitated P with calcium and/or Fe (oxyhydr) oxides (House, 2003; Vilmin et al., 2015). Generally, DIP consists of orthophosphate (PO₄³-), pyrophosphate (pyroP) and polyphosphate (polyP), of which PO₄³⁻ being the most dominant with high reactivity among others, is preferentially utilized by phytoplankton, while some phytoplankton cannot directly assimilate pyroP and polyP (Duan et al., 2016; Diaz et al., 2016). Similar to DIP, recent studies have revealed that phytoplankton or microbial community can also assimilate low molecular weight DOP under special aquatic environmental conditions when DIP is not enough to provide the nutritional needs of living aquatic organisms (Yoshimura et al., 2014; Li et al., 2017). Therefore, information about DOP is also of scientific significance since the extant microorganism community may assimilate DIP and DOP simultaneously, especially if DOP is more abundant and bioavailable relative to DIP in natural waters (Björkman and Karl, 2003). Several factors can influence concentration and distribution of DIP and DOP in coastal waters. For example, the absorbed DIP and DOP on suspended particulate matter (SPM), which is massively transported by rivers and can be desorbed in estuaries and coastal waters due to increasing salinity (Paytan and McLaughlin, 2007; Jordan et al., 2008; Yang et al., 2018a). Studies show that \sim 87% of the particle-bound P in the oceans is delivered through global riverine supply (e.g., Jensen et al., 2006). Because P is highly reactive to water-borne particulate matter, the TPP often accounts for a larger proportion of TP than TDP, especially in turbid (SPM > 100 mg/L) riverine and nearshore waters. Nevertheless, TPP may be an important contributor of dissolved P through desorption processes even in less turbid aquatic environments due to dynamic changes in some physiochemical conditions, and the regeneration or removal of DIP might be related to P partitioning coefficient (K_d) between dissolved and particulate phases (Prastka et al., 1998; Jordan et al., 2008). In summary, particulate P phase can serve as a potential source of DIP and/or DOP for phytoplankton and microbial community growth and metabolism. Thus, knowledge on dissolved and particulate P pool is important to evaluate the transformation potential of P and its bioavailability in estuarine and coastal marine environments.

Maowei Sea (MWS) is a typical subtropical bay influenced mostly by the discharge of the Maolingjiang River and Qinjiang River, and tidal influx from the Beibu Gulf through Qinzhou Bay, and constitutes a unique estuary-bay multi-ecosystem with rich aquatic resources and conducive environment for oyster mariculture (Wei et al., 2017). However, frequent harmful algal blooms have been occurring recently in the MWS due to the rapidly growing industrialization, urbanization, and intense mariculture activities in the watershed (Gu et al., 2015; Zhang et al., 2019). Previous studies in the MWS have focused on sedimentary P (Yang et al., 2019a, 2019b; Dan et al., 2020a). Reports show that inorganic P mainly in the form of Fe-bound P is generally the predominant form of sedimentary P in the MWS, and sedimentary P is dominantly derived from terrestrial sources. Moreover, sediment textural characteristics, distributions of organic matter, hydrodynamics, in addition to external input from agriculture drainage areas and aquaculture activities, together play significant roles for the variation tendencies of different fractions of P in sediments (Yang et al., 2019a, 2019b; Dan et al., 2020a). The potential bioavailable P (i.e., the labile P forms) has been reported to account for more than 70% of the sedimentary TP in the MWS (Yang et al., 2019b). On the other hand, a comprehensive study focusing on P speciation in the water column of Danshuei River Estuary in northern Taiwan, showed that DIP is strongly influenced by desorption from and adsorption onto PIP, of which PIP accounted for ~60% of TP in regions where salinity was <5 psu, but decreased to 40-50% in the lower estuary where salinity exceeded 30 psu (Fang and Wang, 2020). Generally, the spatiotemporal variability in physicochemical factors including pH, salinity, water temperature, SPM in surface water of many coastal marine systems, play different roles on P speciation, distribution, and bioavailability in the water column (Prastka and Malcolm, 1994; Zhou et al., 2016; Shinohara et al., 2018). However, detailed information on the biogeochemistry of P and the transformation behavior between different P species and phases, and their relationships with the spatial distribution of physicochemical parameters and related dissolved nutrients in surface water of the MWS is lacking. Thus, a systematic study into better understanding the biogeochemical behavior of all species of P in the MWS is required given the importance of the MWS and its environmental function for mariculture and fishery resources. Thus, this study was conducted on surface water samples collected along the salinity gradients at the western and eastern flanks of the MWS, which are influenced by the major adjoining river and tributaries. The objectives were as follows. (1) Quantify the abundance of different P species in dissolved and particulate phases in the MWS. (2) Evaluate the dissolved P status in the MWS, and identify the limiting nutrients for primary production based on nutrients molar ratios. (3) Evaluate the relationship between different P species and physiochemical parameters such as salinity, SPM, and Chl-a. (4) Explore the biogeochemical changes and partitioning of P between dissolved and particulate phases. (5) Apply a two-end-member mixing model to elucidate the influence of freshwater discharge on P removal/addition.

2. Materials and methods

2.1. Study area

The MWS is a semi-enclosed bay in the northern Beibu Gulf, situated at the northwestern part of South China Sea (Wang et al., 2017; Dan et al., 2020a) (Fig. 1a). The surface area of the MWS is approximately 135 km^2 and the water depth is relatively shallow (average $\sim 2.5 \text{ m}$; Liu et al., 2016; Gu et al., 2018). The regional climate is controlled by the

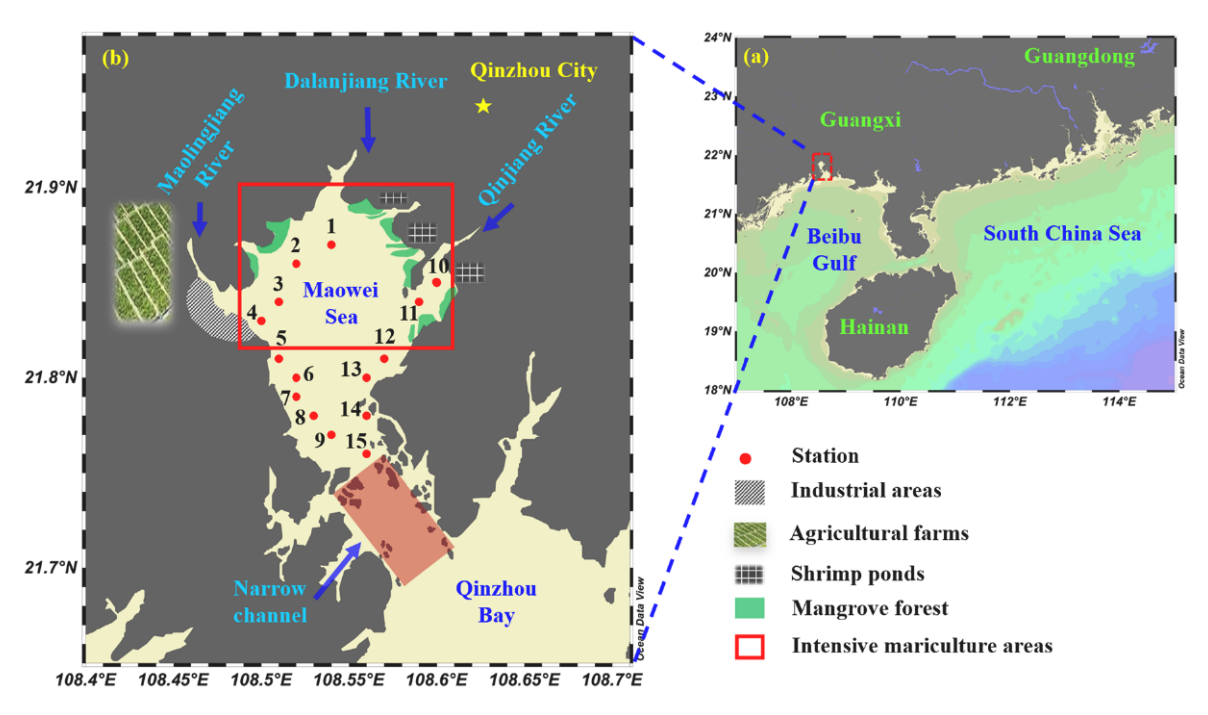


Fig. 1. Map of (a) the study location and (b) sampling sites in the Maowei Sea, northern Beibu Gulf.

tropical maritime monsoon with annual air temperature ranging from $\sim\!0.8\,^{\circ}\text{C}$ to 37.4 $^{\circ}\text{C}$, with an average of 22.1 $^{\circ}\text{C}$. The mean annual rainfall is 2140 mm, of which 80-85% falls during the rainy season (from May to September) (Meng et al., 2016; Chen et al., 2018). The annual freshwater discharge from the Maolingjiang River and Qinjiang River (the two largest rivers in the MWS situated at the western and eastern flanks, respectively) is 25.9 \times 10⁸ m³ y⁻¹ and 20.3 \times 10⁸ m³ y⁻¹, respectively. The main stream length of Dalanjiang River is ~21.33 km and its catchment area is only 62.3 km², with a low freshwater discharge. About $8.6 \times 10^4 \text{ tons y}^{-1}$ of suspended sediment is co-delivered from these rivers into the MWS (Chen et al., 2018). Irregular diurnal tides (average tidal range ~2.5 m) exist along the coast with a maximum tidal elevation of 5.5 m (Tian et al., 2014; Chen et al., 2018). The surface water circulation in the MWS is anticyclonic, and the water current from Qinzhou Bay enters and exit from the eastern and western coastal areas, respectively (Xu et al., 2020). The baggy geomorphology of MWS together with the narrow outlet channel linking it with the Qinzhou Bay somewhat limits rapid water exchange between these two water bodies and Beibu Gulf (Zhang et al., 2019). This condition makes the MWS behaves like a typical subtropical estuary, especially during the summer rainy season with surface salinity being generally <20 psu. Urban settlements dominate land use in the MWS watershed, and most of the northern regions are dominated by shrimp ponds. The eastern catchment regions are also dominated by shrimp ponds, including agricultural activities and mangrove forest, while factories and agricultural farms are clustered around the western regions. The natural mangrove reserve wetlands occupy an area of \sim 2784 hm² along the coastline of the MWS. The human population within 1–15 km of the region where the MWS is located as of 2016, was ~0.45 million inhabitants, which represents ~10% of the total Qinzhou population in the Guangxi province in China. The MWS is the largest natural oyster seedling and mariculture bay in China and the mangrove nature reserve is the most extensive in Qinzhou Bay. The sea represents a significant economic developing region, which has been gradually impacted by anthropogenic activities (Gu et al., 2018).

2.2. Sampling

Field survey was carried out in July 2018. Fifteen representative

sampling stations were selected longitudinally along the salinity gradients starting from the northern and ending at the southern regions where the MWS connects with the Qinzhou bay (Fig. 1b). The sampling stations consisted of nine sites (1-9) at the western flank of the Sea and six sites (10-15) at the eastern flank (Fig. 1b). The rational for selecting these sites was to capture the influence of the adjoining rivers such as the Maolingjiang River and/or the Dalanjiang River at the western flank of the Sea, and Oinjiang River at the eastern flank on biogeochemical behavior, transformation, and speciation of P in the MWS. Considering that physicochemical factors (such as salinity) are greatly affected by tidal fluctuations, the sampling was conducted simultaneously during the same tide time at the western and eastern flanks. At each site, surface water samples (<1 m below surface) were collected using Niskin bottle water sampler (volume ~5 L) and stored in pre-acid-cleaned 2 L HDPE plastic bottles. In order to limit the possible changes in P species in the samples over time, the collected samples were immediately stored in cooling container (temperature < 4 $^{\circ}$ C) in the field sampling. Physical parameters such as surface water salinity (S), temperature (T), pH and dissolved oxygen (DO), were measured in situ using a pre-calibrated multi-parameter water quality probe (AP-5000, Aquaread Co., UK), while the oxidation-reduction potential (Eh) was also measured in situ using a portable redox potentiometer (Thermo Fisher 4-Star, USA). In the laboratory, 300 mL of the water samples were filtered through precombusted 0.45 µm Nuclepore filters (Whatman, 47 mm) for the measurement of dissolved nitrite (NO₂), nitrate (NO₃), ammonium (NH₄⁺), total dissolved N (TDN), dissolved silicate (DSi), TDP and DIP. The suspended solids retained on the filters were used for the measurement of SPM, TPP, and PIP concentrations. Additionally, aliquot of 500 mL water samples was also filtered through pre-combusted 0.7 µm GF/F filters under low vacuum for chlorophyll a (Chl-a) analyses. All sampling pretreatment were completed within 5 h. The filtrates and filters were immediately preserved at -20 °C in the laboratory until further analyses, which were subsequently done within one month.

2.3. Laboratory analyses

Concentrations of NO_2^- were measured by reacting NO_2^- with aromatic amine, while NO_3^- and NH_4^+ determinations were based on copper-cadmium (Cu-Cd) column reduction and indophenol blue color

formation methods, respectively. The sum of NO_2^- , NO_3^- , and NH_4^+ is hereafter reported as dissolved inorganic N (DIN). DSi was measured using a reducing reagent, molybdate and oxalic acid. The reaction products were quantified using the modified spectrophotometric methods of Hansen and Koroleff (1999). Concentrations of NO_2^- , NO_3^- , NH_4^+ and DSi were determined in the laboratory using an auto analyzer (AA3 HR, Seal Analytical Ltd., UK). TDN was decomposed to NO_3^- with boric acid-persulfate oxidation solution ($K_2S_2O_8$ and H_3BO_3 in NaOH solution). This was done in an autoclave at 120 °C for 0.5 h, and then measured using an auto analyzer (Liu et al., 2005; Lin et al., 2012). Concentrations of dissolved organic nitrogen (DON) was calculated as the difference between TDN and DIN (i.e., DON = TDN – DIN). The analytical precision was < 5% for nutrients mentioned above (Yang et al., 2018a).

The determination of TDP was based on an autoclave-assisted acid persulfate method with modification according to Lin et al. (2012). In brief, 10 mL of the filtered water sample and 1 mL of acidified $K_2S_2O_8$ solution (50 g/L, pH = 1) were added to a plug colorimetric tube, and the mixed solution was digested at 140 °C for 4 h in an autoclave, followed by measurements using the spectrophotometric phosphomolybdate blue method (Lin et al., 2016). Concentrations of DIP were directly determined without digestion, and the amount of DOP was acquired from the difference between TDP and DIP. The detection limit was generally between 8 and 10 nM based on replicate blank sample measurements, with a precision <2% for both TDP and DIP at 0.1 μM level. TPP was measured following high temperature combustion and acid hydrolysis of the filters as described by Solórzano and Sharp (1980) with some improvements by Zhang et al. (2010). Briefly, the filters were wetted with 0.5 M MgCl₂ solution and heated in a drying oven at 95 °C until dryness and then organic P compounds were decomposed by ashing in a furnace at 550 °C for 2 h. The residue was extracted with 1 M HCl solution at room temperature for 24 h. The sample for PIP was also extracted using 1 M HCl solution at room temperature for 24 h (Aspila et al., 1976). After neutralization and dilution, both extractions of TPP and PIP were quantified following the DIP method. Concentrations of POP were obtained by subtracting PIP from TPP (Cai et al., 2008). The analytical precision for TPP and PIP were <1%.

Concentrations of SPM were determined by finding the weight difference between the particulate matter retained on the dried filters and blank filters before filtration. The filter samples were dried to constant weights and reweighed, and the levels of SPM were calculated from net dry weights and filtered water sample volumes according to Lin et al. (2016) and Dan et al. (2019). Chl-a was extracted in 10 mL 90% (v/v) HPLC-grade acetone in the dark at 4 °C for 24 h, and measured using a fluorescence spectrophotometer (F-4500, Hitachi Co., Japan) after centrifugation (Parsons et al., 1984). Instrument calibration was done with Chl-a standard from spinach (Sigma-Aldrich C5753). The analytical precision for Chl-a was <3% (Yang et al., 2018a).

2.4. Distribution coefficient

The partitioning of P between dissolved and particulate phases can be quantified using the conditional distribution coefficient (K_d). Due to the proportional differences in P phases in this study, the P data for the western and eastern flanks were pooled together to calculate K_d in order to fully comprehend the biogeochemical behavior of P in surface water of the MWS (Turner, 1996; Prastka et al., 1998; Lin et al., 2012). The K_d is given as follows:

$$K_d = \frac{C_p}{C_d \cdot [SPM]} \tag{1}$$

where C_p and C_d are the concentrations of particulate and dissolved P (all in μM including inorganic and organic P pools), respectively. [SPM] is the concentration of suspended particulate matter (g/mL). Therefore, the dimension of K_d is in mL/g, and the value of K_d is expressed as log

(K_d) (Lin et al., 2013).

2.5. Two-end-member mixing model

The two-end-member mixing model was built on mass balance equations for salinity and the component of two water masses (Li et al., 2017; Yang et al., 2018a):

$$f_1 + f_2 = 1 (2)$$

$$S_1 f_1 + S_2 f_2 = S {3}$$

where f_1 and f_2 represent the fractions of the freshwater and seawater end-members, respectively. S_1 and S_2 represent the salinity of the two end-members. Thus, the prediction of the specific P concentration $(P_{\rm m})$ was based on the two end-member model calculated as follows:

$$P_m = P_1 f_1 + P_2 f_2 \tag{4}$$

where P_1 and P_2 are the specific P concentration of the two endmembers, respectively. The difference between the predicted value and the ambient value is defined as ΔP , and calculated following equation below:

$$\Delta P = P_m - N \tag{5}$$

where N is the value of the ambient phosphorus concentration in the water sample. A negative ΔP value implies DIP addition, while a positive value indicates DIP removal. Here, it is important to emphasize that there are some limitations in the use of the binary mixing model in this study. First, the salinity of the freshwater endmember (S_1) does not truly represent the freshwater salinity. Normally, this condition would have been met at the upstream regions beyond tidal reversal. Secondly, the salinity of the saltwater end-member (S_2) during this study (see Table 1) appears to be largely influenced by continuous freshwater supply and limited salt-water influx from the Beibu Gulf to the MWS. Thus, it is possible that the near freshwater conditions (i.e., western flank site 1 and eastern flank site 10) at the norther regions during this study (summer wet season) may change at other seasons when there is a reduced riverine freshwater outflow and enhanced saltwater influx. Apparently, the lower salinity of the starting sampling sites at each flank of the MWS was an average value measured during the flood and ebb tides during this study. Thus, this allows the evaluation of the influence of riverine influx on the bioavailability of DIP, whereby the deviations maybe somewhat subject to some sort of non-conservative processes at the western and eastern flank of the MWS during the wet summer

2.6. Statistical analysis and graphing

Data analysis was done using the Statistical Program for the Social Science (SPSS) (Version 22.0; SPSS Inc., IBM, Armonk, NY, USA). Here, one-way analysis of variance (ANOVA) was used to evaluate whether the difference in the mean level of the studied parameters between the western and eastern flanks was statistically significant at 95% confidence limit. Data normality was checked using Kolmogorov-Smirnov and Shapiro-Wilk test. Pearson's correlation analysis with a two-tailed test of significance (99% and 95% confidence interval) was done to evaluate the relationship of the measured physicochemical parameters and P species. Plots showing the distributions of the measured parameters were produced using Origin 9.0 (OriginLab, USA), while the map of the study area showing the sampling sites were produced using Ocean Data View (ODV Version 5.2.1) software (Sclitzer, Reiner, Ocean Data View, https://odv.awi.de, 2020).

Table 1
Sampling locations, sites, and physicochemical properties at the western and eastern flanks of the Maowei Sea (MWS).

Sample Locations	Sites	Longitude (°E)	Latitude (°N)	T (°C)	S (psu)	pH	DO (mg/L)	Eh (mV)	Chl- a (µg/L)	SPM (mg/L)
Western flank	1	108.54	21.87	30.6	0.63	8.48	6.37	63	1.95	42
	2	108.52	21.86	29.9	0.65	8.98	6.01	65	3.18	88.3
	3	108.51	21.84	30.1	1.02	8.98	6.44	60	2.13	57
	4	108.5	21.83	29.6	1.76	8.08	6.15	106	3.87	34.7
	5	108.51	21.81	29.8	2.6	8	6.11	81	4.68	35.7
	6	108.52	21.8	29.8	3.02	7.86	6.16	49	4.59	39
	7	108.52	21.79	29.7	5.39	8.02	5.86	115	3.27	40.3
	8	108.53	21.78	29.8	9.35	7.97	5.63	158	6.63	48.4
	9	108.54	21.77	30.1	15.07	8.19	5.52	183	7.95	39
Eastern flank	10	108.6	21.85	30	1.17	7.46	6.34	73	1.32	31
	11	108.59	21.84	30.1	3.93	8.13	6.17	98	5.22	30.8
	12	108.57	21.81	30	10.33	7.76	5.65	152	2.64	36.7
	13	108.56	21.8	30.2	10.96	8	5.76	70	5.1	42
	14	108.56	21.78	30.1	13.02	8.89	5.66	129	7.35	48.5
	15	108.56	21.76	30.3	17.96	8.33	5.72	29	5.91	57.7

3. Results

3.1. Physicochemical parameters

The levels and distributions of physicochemical parameters in surface water are presented in Table 1 and Fig. S1a-d. Salinity ranged from 0.63 to 15.07 psu at the western flank, and 1.17-17.96 psu at the eastern flank, and showed an obvious increasing trend from the northern to the southern regions of the MWS at both blanks (Fig. S1a). pH at the western and eastern flank ranged from 7.86–8.98 (average, 8.28 \pm 0.43) and 7.46–8.89 (average, 8.10 ± 0.49), respectively. Although pH showed a general decreasing trend from site 1 to site 6, and then increased to site 9 at the western flank, its distributional trend at the eastern flank generally increased from the northern region to the southern region (Fig. S1b). Eh ranged from 49–183 mV (average, 98 \pm 47 mV) and 29–152 mV (average, 92 \pm 44 mV) at the western and eastern flanks, respectively, suggesting that the surface water in MWS was somewhat oxidative during this study (Fig. S1c). The levels of SPM ranged from 34.7 to 88.3 mg/L (average, 47.2 \pm 16.9 mg/L) at the western flank and 31.0 to 57.5 mg/L (average, 41.1 \pm 10.6 mg/L) at the eastern flank. High variability in SPM was observed at the northern regions between sites 1-4 at the western flank where salinity was <5 psu, but remained somewhat stable at higher salinity sites (Fig. S1d). Water temperature ranged from 29.6 °C–30.6 °C (average, 29.9 \pm 0.30 °C) at the western flank, and 30.0 °C–30.3 °C (average, 30.1 \pm 0.12 °C) at the eastern flank, and the distributional patterns were somewhat similar to that of SPM, especially at the eastern flank (Fig. S1e). The level of Chl-a ranged from $1.95-7.95~\mu g/L$ (average, $4.25~\pm~1.99~\mu g/L$) at the western flank and $1.32\text{--}7.35~\mu\text{g/L}$ (average, $4.59~\pm~2.21~\mu\text{g/L}$) at the eastern flank. The distributional patterns of Chl-a at the western and eastern flanks were similar, showing a progressive increasing trend (Fig. S1f) as salinity increases from the northern to the southern regions of the MWS. DO ranged from 5.52-6.44 mg/L (average, 6.03 \pm 0.31 mg/L) and 5.65–6.34 mg/L (average, 5.88 \pm 0.30 mg/L) at the western and eastern flanks respectively, showing that the surface water in MWS is well oxygenated. The distributional trends decreased from the northern to the southern region of the MWS at both flanks (Fig. S1g). Generally, there was no significant difference (ANOVA, p > 0.05) in the mean levels of the physicochemical parameters between the western and eastern flanks of the MWS during this study.

3.2. Distributions of DIN, DON and DSi

The concentrations and distributions of DIN and DSi in surface water at the western and eastern flanks of the MWS are shown in Table S1, Fig. S1h and in Fig. S2a–b, respectively. There was a significant variation (ANOVA, p < 0.05) in the mean concentration of DON, with exception of DIN and DSi between the western and eastern flanks of the

MWS. DIN ranged from 22.77 to 81.32 μM (average, 41.64 \pm 16.92 $\mu M)$ and 32.69–80.02 (49.2 \pm 18.0 $\mu M)$ at the western and eastern flanks, respectively. DIN was the major form of TDN at both flanks (Fig. S2c-d), and its concentration trend gradually decreased with an increasing salinity from the north to south in the MWS (Fig. S2a). Among the different DIN species, NO₃ was the dominant form, which singly accounted for 42.4% and 54.7% of TDN in the western and eastern flanks, respectively (Fig. S2c-d). DON accounted for 44.7% of TDN in the western flank, which was higher than average contribution (23.3%) of DON to TDN at the eastern flank (Fig. S2c-d). Although the surface water SPM during this study was generally <100 mg/L, the elevated NO₃ in the MWS, may be related to slow nitrification process as NH₄ and NO₂ averagely accounted for <30% of the DIN at both flanks during this study. Moreover, short-term localized nitrification process may have accounted for lower DON concentrations compared to NO₃ at the eastern flank. The concentrations of DSi ranged from 7.40–41.01 μM (average, $23.58 \pm 11.32~\mu\text{M})$ and 7.21–34.20 μM (average, 25.27 \pm 11.70 $\mu\text{M})$ at the western and eastern flanks of the MWS, respectively, and showed a gradually decreasing trend with increasing salinity from the northern to the southern regions of the MWS (Fig. S1h). While the distribution of DSi appears to be dominantly influenced by land-based sources, dissolved N species tends to be influenced by both terrestrial input and biogeochemical processes within the MWS. Similar trends have been reported in the Dafengjiang River estuary in the northern Beibu Gulf (Yang et al., 2018a).

3.3. Distributions of dissolved P and molar ratios

Concentrations of DIP, DOP and TDP in the MWS are presented in

Table 2The levels of phosphorus in dissolved and particulate phases in surface water at the western and eastern flanks of the Maowei Sea (MWS).

Sample Locations	Sites	DIP (μM)	DOP (μM)	TDP (μM)	PIP (μM)	POP (μM)	TPP (μM)	TP (μM)
Western flank	1	1.88	2.45	4.33	3.13	0.71	3.84	8.17
	2	4.04	0.79	4.83	2.97	1.16	4.13	8.96
	3	1.76	1.25	3.01	2.12	0.88	3	6.01
	4	1.15	2.1	3.25	1.3	0.42	1.72	4.97
	5	0.94	3.12	4.06	1.34	1.2	2.54	6.6
	6	1.52	1.68	3.2	1.81	0.63	2.44	5.64
	7	1.09	2.2	3.29	1.3	0.57	1.87	5.16
	8	0.71	4.05	4.76	0.93	0.65	1.58	6.34
	9	1.33	2.2	3.53	0.84	0.61	1.45	4.98
Eastern flank	10	2.43	1.02	3.45	1.71	0.66	2.37	5.82
	11	1.4	3.04	4.44	1.13	0.46	1.59	6.03
	12	1.41	1.61	3.02	0.91	0.37	1.28	4.3
	13	1.46	2.08	3.54	0.82	0.41	1.23	4.77
	14	0.86	3.71	4.57	0.82	0.73	1.55	6.12
	15	0.91	2.77	3.68	1.16	0.28	1.44	5.12

Table 2. The distributional trends are depicted in Fig. 2a-b, and Fig. 2e–f. No significant differences (ANOVA, p > 0.05) was observed in the mean level of dissolved P, except for DOP between the western and eastern flank of the MWS. DIP ranged from 0.71-4.04 µM (average, 1.60 \pm 0.99 $\mu M)$ and 0.86–2.43 μM (average, 1.41 \pm 0.56 $\mu M), while DOP$ ranged from 0.79–4.05 μM (average, 2.20 \pm 0.97 $\mu M)$ and 1.02–3.71 μM (average, $2.37 \pm 0.99 \,\mu\text{M}$) at the western and eastern flanks of the MWS, respectively. Generally, decreasing DIP concentrations with increasing salinity from the northern to the southern regions of the MWS were observed at both flanks (Fig. 2a-b). The average concentrations of DOP at both flanks were somewhat comparable, but the distributions were highly variable, showing an increasing tendency as salinity increases from the north to south in the MWS (Fig. 2a-b). The distributions of dissolved P forms (i.e., DIP and DOP) in this study are consistent with the observations in Jiulong River Estuary (Lin et al., 2013). The concentration of TDP ranged from 3.01–4.83 μ M (average, 3.81 \pm 0.70 μ M) and 3.02–4.57 μM (average, 3.78 \pm 0.60 $\mu M)$ at the western and eastern

flanks, respectively. At the western flank, TDP had first decreased from 4.33 μ M (salinity, \sim 0.63 psu) at site 1 to 3.01 μ M (salinity, 1.02 psu) at site 3, varied from 3.20–4.06 μM at sites 4–7 (salinity, 1.76–5.39 psu), then increased to 4.76 μ M (salinity, \sim 9.00 psu), and finally decreased to 3.50 μ M at site 9 (salinity, ~15.00 psu) (Fig. 2e). The average concentrations of TDP at both flanks were comparable, probably due to similar DOP levels. The levels of DIP and DOP in the TDP pool varied widely across the investigated sites at each flank. DIP and DOP accounted for 14.9–83.6% (average, 41.9 \pm 20.2%) and 16.4–85.1% (average, 58.1 \pm 20.2%) (Fig. 3a), and 18.8–70.4% (average, of 38.9 \pm 18.5%) and 29.6–81.2% (average, 61.1 \pm 18.5%) (Fig. 3b) of the TDP pool at the western and eastern flanks, respectively. Considering the entire dataset in this study, the molar DIN/DIP ratios ranged from 12 to 68 (average, 33 \pm 13), DSi/DIN ratios varied from 0.16–0.96 (average, 0.57 \pm 0.27), while DSi/DIP ratios ranged from 6–26 (average, 17 \pm 6) (Fig. 4). This stoichiometric relationship between DIN and DSi, with DIP have important implication for the plankton community, which may also

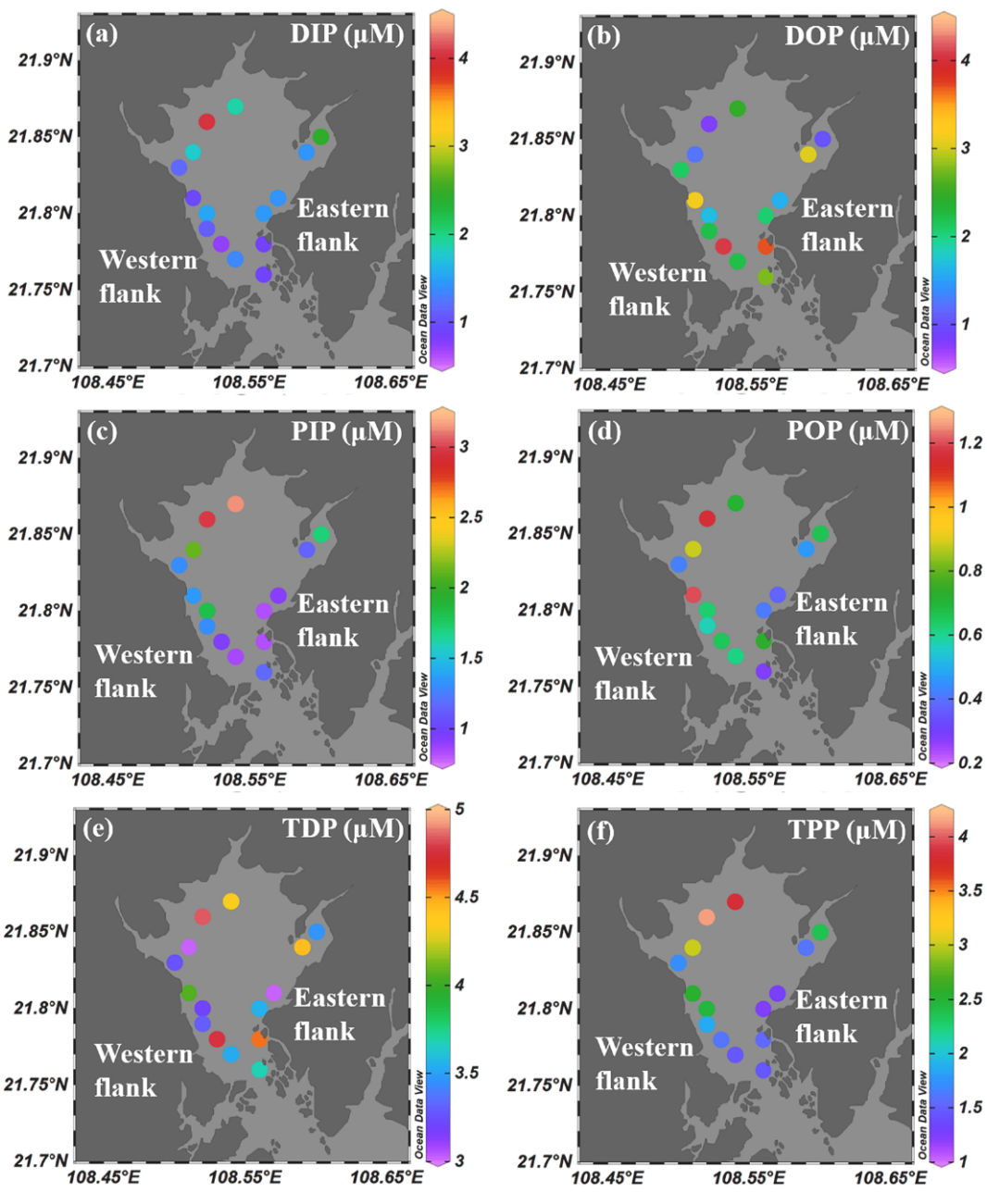


Fig. 2. Spatial distributions of different phosphorus species along the salinity gradients in surface water at the western and eastern flanks of the Maowei Sea.

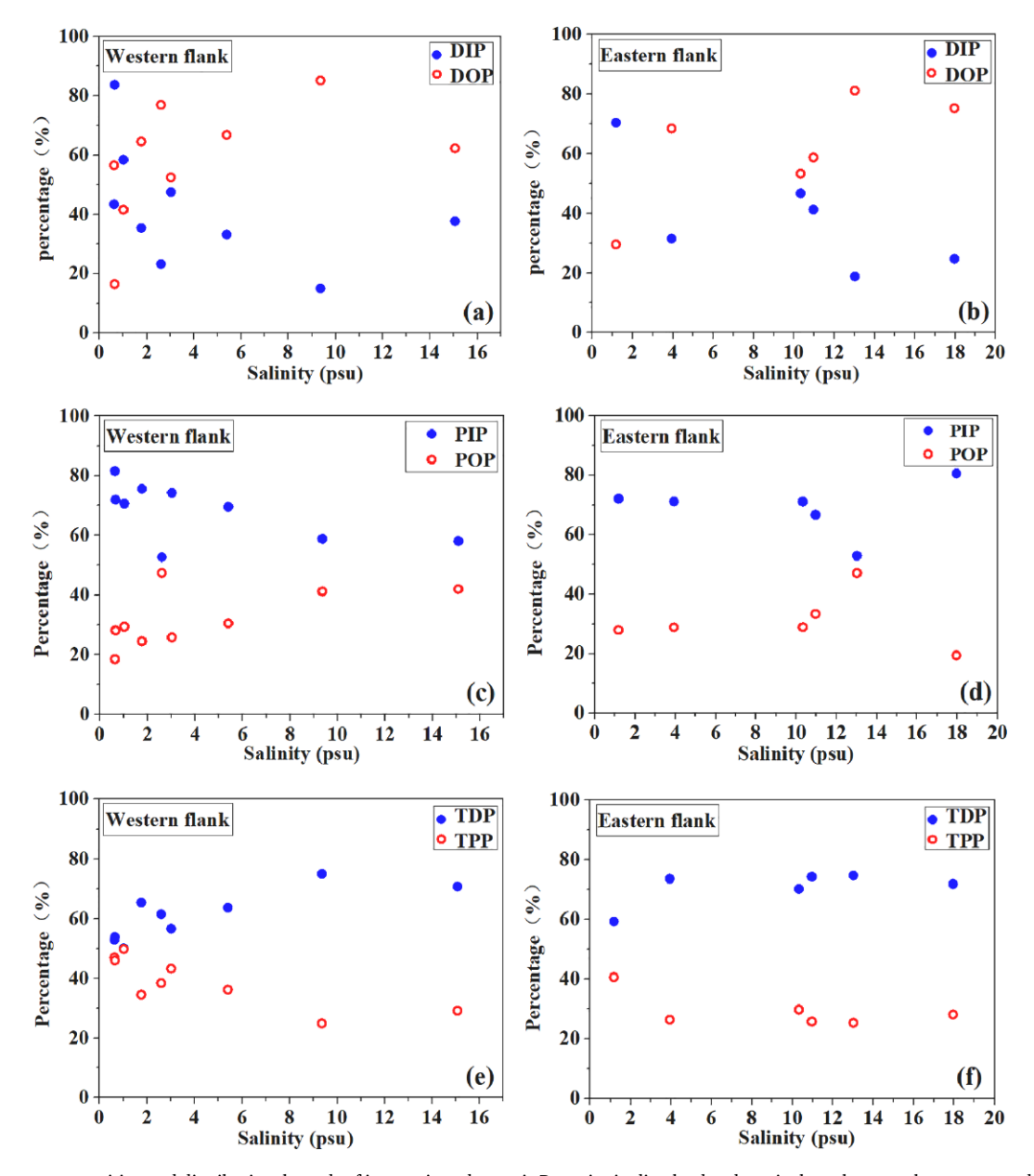


Fig. 3. Surface water composition and distributional trends of inorganic and organic P species in dissolved and particulate phases at the western and eastern flanks of the Maowei Sea.

serve as an indicator for the evaluation of nutrient limitation in the $\ensuremath{\mathsf{MWS}}.$

3.4. Spatial variations of particulate inorganic and organic P

The concentration and distribution of various particulate P species are presented in Table 2, Fig. 2c–d. Just like the dissolved P phase, there was no significant variation (ANOVA, p>0.05) in the mean concentration of particulate P except for POP, between the western and eastern flanks of the MWS. The concentration of PIP ranged from $0.84–3.13~\mu\text{M}$ (average, $1.75\pm0.84~\mu\text{M}$) and $0.82–1.71~\mu\text{M}$ (average, $1.09\pm0.34~\mu\text{M}$), while POP ranged from $0.42–1.16~\mu\text{M}$ (average, $0.76\pm0.27~\mu\text{M}$) and $0.28–0.73~\mu\text{M}$ (average, $0.49\pm0.17~\mu\text{M}$) at the western and eastern flanks, respectively. The distributional trend of PIP at the western flank is similar to that at the eastern flank, which showed a generally decreasing trend as salinity increases from the north to south in the MWS (Fig. 2c–d). Slight changes were observed in the distributional trend of PIP at the eastern flank. At first, PIP showed a decreasing trend as

salinity increases, and then slightly increased at the higher salinity sites 14 and 15 (Fig. 2d), which also corresponded with sites where elevated SPM levels were recorded at the eastern flank (Fig. S1d). POP varied minimally with no distinctive trend in its distribution patterns at both flanks (Fig. 2c–d). TPP concentrations ranged from 1.45–4.13 μM (average, 2.51 \pm 0.98 μM) and 1.23–2.37 μM (average, 1.59 \pm 0.41 μM), and showed a gradually decreasing trend at the western flank and eastern flank, respectively. Within the particulate P pool, PIP dominated the particulate P phase, accounting for 68.1 \pm 9.5% and 69.1 \pm 9.1% (Fig. 3c), while POP only accounted for 31.9 \pm 9.5% and 30.9 \pm 9.1% at the western flank and eastern flank (Fig. 3d), respectively.

Considering both dissolved and particulate P phases, dissolved P was the predominant phase in the total P pool, accounting for 61.1% and 70.7%, while particulate P only accounted for 38.9% and 29.3% at the western flank and eastern flank (Fig. 5), respectively. As the salinity increased, the increasing TDP/TP ratios in the surface water were comparable to the decreasing in TPP/TP ratios at the western flank (Fig. 3e) and eastern flank (Fig. 3f), suggesting a transformation of P

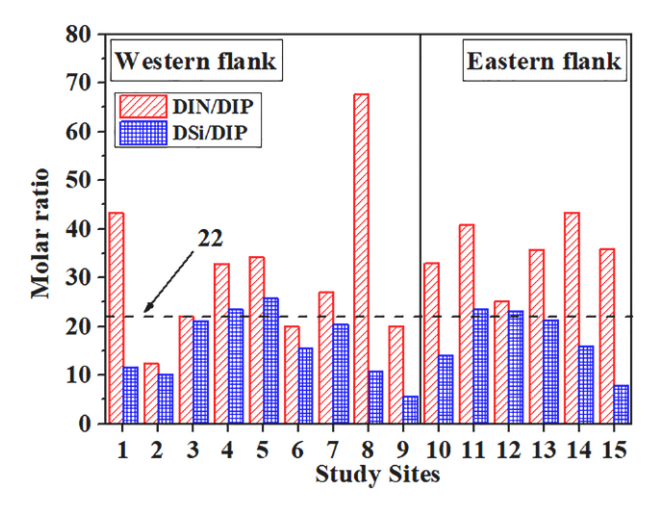


Fig. 4. Molar ratios of dissolved inorganic nitrogen and dissolved silica to dissolved inorganic phosphorus as shown by the red and blue bars, respectively along the investigated sites in the Maowei Sea. The black dashed line indicates DIP bio-limitation when DIN/DIP and DSi/DIP > 22 (Justić et al., 1995). (For interpretation of the references to color in this figure legend, the reader is referred to the web version of this article.)

between dissolved and particulate phases in surface water of the MWS. In addition, the partitioning of P between dissolved and particulate phases was quantitatively evaluated using its distribution coefficient (K_d). Considering the entire dataset, the $P\log(K_d)$ values obtained for the MWS ranged from 3.83 to 4.34 with an average of 4.09 \pm 0.18 (Fig. 6a). The average $P\log(K_d)$ in this study is slightly lower compared to values reported for other study areas such the Bay of St. Louis (4.96, Lin et al., 2012), Jiulong River Estuary (4.57, Lin et al., 2013) and Pearl River Estuary (4.51, Li et al., 2017).

4. Discussion

4.1. Dissolved inorganic and organic P status and nutrient ratios

The levels of DIP and DOP in MWS during this study in comparison with other worldwide estuaries and bays are presented in Table 3. It is important to highlight here that escalated anthropogenic activities have resulted in many reported cases of aquatic environmental degradation (e.g., Zhang et al., 2015; Wang et al., 2020a, 2020b), and are responsible for the alteration of the global biogeochemical cycles in recent years.

The effects of land-use change on the remobilization of P including the rate at which inorganic fertilizer is widely used for agricultural practices in many watersheds, soil erosion, and local sewage discharge, have significantly increased the tons of P and the frequency of algal outbreak and eutrophication in estuaries and marginal seas (Mackenzie et al., 2002; Zhang et al., 2016). Many estuaries and coastal water experiences occasional and/or frequent algal bloom and eutrophication due to increasing human impacts in Chinese coastal regions (Duan et al., 2008; Pan and Wang, 2012; Yan et al., 2012). Concentrations of DIP in eutrophic aquatic systems exceed 0.1 mg L^{-1} (i.e., $> 3.2~\mu M$), and exceeds the proportions of DOP in the TDP pool (Lemley et al., 2015). Examples of such eutrophic aquatic systems are the Scheldt Estuary (van der Zee et al., 2007), Jiulong River Estuary (Lin et al., 2013), and Danshuei River Estuary (Fang and Wang, 2020) (Table 3), where elevated DIP concentrations have been heavily attributed to anthropogenic input (Alvarez-Vazquez et al., 2016). However, there are other eutrophic aquatic systems such as the Pearl River Estuary (Lu et al., 2009) and the Nile River Estuary (Abdel-Satar et al., 2017), where DOP dominates the TDP pool. Although rivers and/or ground waters are the main sources of terrestrial dissolved nutrients in estuaries and coastal waters, studies have shown that elevated DOP or DON pools are also largely delivered from natural sources in coastal waters (e.g., Dan et al., 2019; Wang et al., 2020a, 2020b). Thus, the amount and characteristics of dissolved inorganic or organic P in most estuaries and coastal marine systems may not entirely depend on anthropogenic perturbations, but on autochthonous sources as well as the economic functionality of an aquatic system.

As shown in Table 3, the concentrations of DIP in the MWS were lower to medium range compared to other aquatic systems in different regions, while DOP was generally higher than other referenced systems. It is important to note that P is mostly adsorbed by soil particles and SPM, and the adsorption capacity may increase as the levels of Fe (oxyhydr) oxides, calcium, aluminum and/or organic matter increases in waters. Particularly, the presence of Fe (oxyhydr) oxides or biogenic apatite effectively limits the dissolution of P and its availability in the water column (Liu et al., 2004). Lower concentrations of DIP in many Chinese coastal waters have been attributed high adsorption on particulate matter (e.g., Liu et al., 2009). Moreover, China is the largest mariculture producer in the world, with an annual production of ~17 million tons (Mt) of seaweed and shellfish mariculture (MOAC, 2017), and MWS is the largest oyster mariculture bay in southwest China. Therefore, elevated surface water DOP would be expected in most of the Chinese coastal waters, including mariculture bays due to biological productions. Although eutrophication occasionally occurs in the MWS,

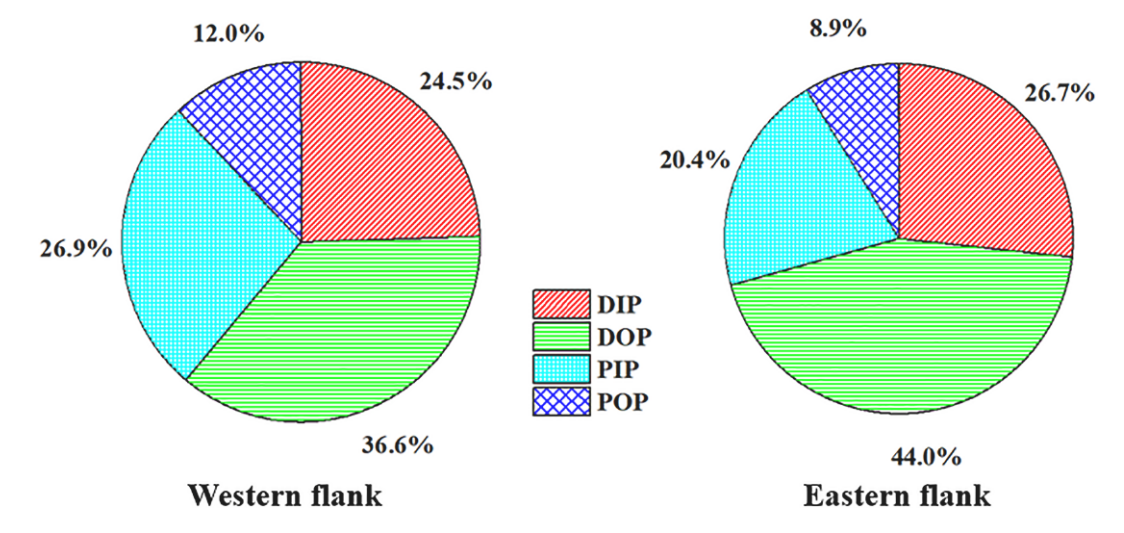


Fig. 5. Surface water proportions of dissolved inorganic P (DIP), dissolved organic P (DOP), particulate inorganic (PIP) and organic P (POP) in total P (TP) pool at the western and eastern flanks of the Maowei Sea.

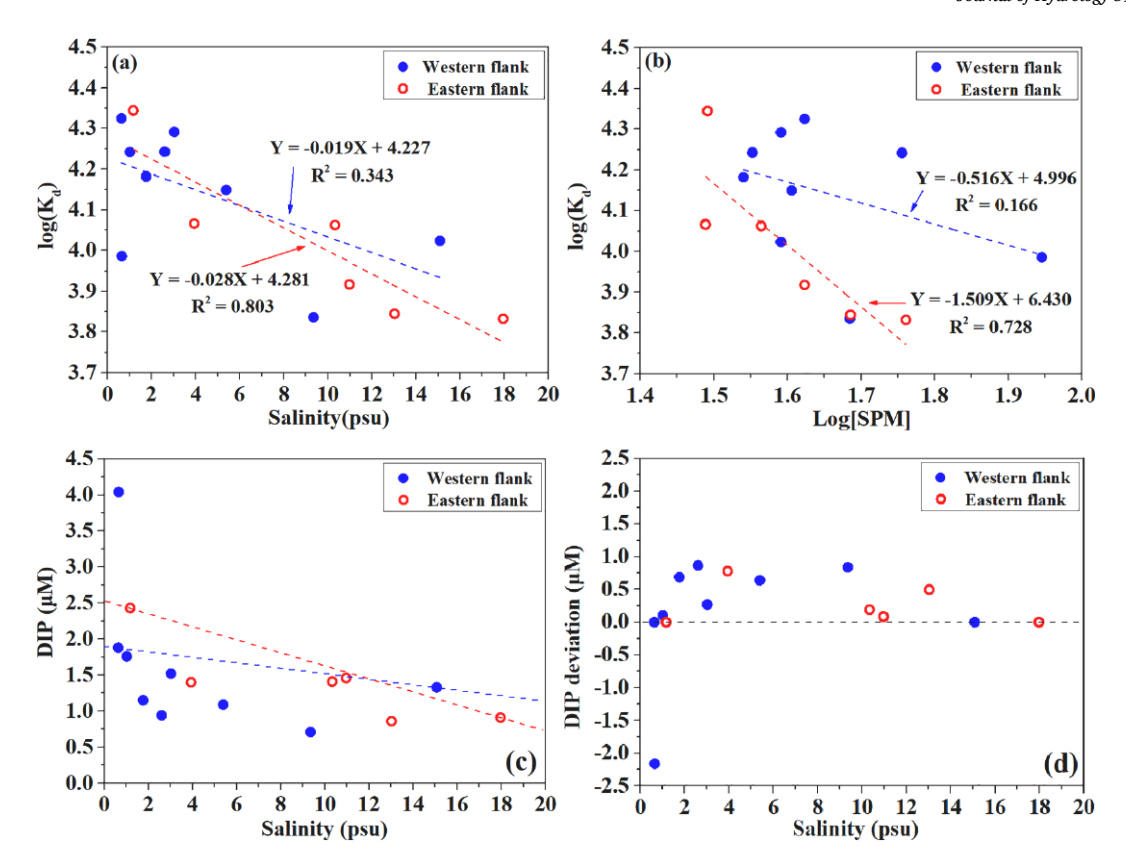


Fig. 6. The surface water phosphorus partitioning coefficients [log(Kd)] against salinity gradients (a) and log[SPM] (b), as well as theoretical mixing (c) and deviations of DIP (d) against salinity based on two-end-member mixing model at the western and eastern flanks of the Maowei Sea.

 Table 3

 The levels of phosphorus in dissolved and particulate phases in surface water of the Maowei Sea (MWS) compared to other estuarine and coastal systems.

Study Area	DIP (μM)	DOP (µM)	PIP (μM)	POP (μM)	Reference		
Scheldt estuary	3.3	0.7	4	1.2	Van der Zee et al., 2007		
Fox River	0.83 (0.68-0.98)	0.60 (0.52-0.68)	0.96 (0.87-1.05)	1.02 (0.73-1.31)	Ho et al., 2010		
Mississippi River	2.89 (2.07-4.20)	0.35 (0.21-0.45)	3.45	1.81	Cai and Guo, 2009; Shim et al., 2012		
Bay of St. Louis	0.15 (0.02-0.44)	0.26 (0.17-0.52)	0.23 (0.06-0.39)	0.62 (0.28-0.94)	Lin et al., 2012		
Jiulong River estuary	1.20 (0.52-2.14)	0.57 (0.47-0.62)	1.35 (0.12-4.38)	0.59 (0.09-1.81)	Lin et al., 2013		
North Yellow Sea	0.10 (0.01-0.34)	0.68 (0.01-2.20)	0.15 (0.07-0.33)	0.08 (0.03-0.15)	Duan et al., 2016		
Chukchi Sea	0.89	0.49	0.08	0.06	Piper et al., 2016		
Green Bay	0.03 (0.01-0.11)	0.17 (0.06-0.27)	0.08 (0.01-0.16)	0.05 (0.02-0.10)	Lin et al., 2016		
Milwaukee River	1.81 (0.69–3.05)	0.54 (0.11-0.91)	0.58 (0.40-0.71)	0.68 (0.34-1.03)	Lin and Guo, 2016		
Pearl River estuary	1.44	0.58	0.78	0.83	Li et al., 2017		
Jiaozhou Bay	0.27	0.31	0.12	0.16	Yuan et al., 2018		
Danshuei River estuary	0.37-3.18	0.62-1.15	0.14-1.78	0.19-0.64	Fang and Wang, 2020		
Maowei Sea (MWS)	1.53 (0.71-4.04)	2.27 (0.79-3.71)	1.49 (0.82-3.13)	0.65 (0.28-1.16)	This study		

the overall contribution of DIP to surface water eutrophication in the MWS seems less even as anthropogenic input may have accounted for the elevated DIP, which exceeded the threshold for eutrophication at the western flank site 2 (Table 2; Fig. 2a). In summary, it is likely that the higher proportions of DOP compared to DIP in the MWS, and the difference in the concentrations of dissolved P between the MWS and other aquatic systems in the literature may be attributed to different sources of P within the watershed, the level of biological productivity and biogeochemical processes influencing P concentrations and dynamics.

Generally, phytoplankton growth rate can be limited by one or more essential macronutrients. Thus, the control of primary production by nutrients has occasioned much research on the metabolic characteristics of phytoplankton in many freshwater and coastal marine ecosystems. Because DIN, DIP, and DSi can stimulate phytoplankton blooms, including harmful algal bloom species (HABs), in coastal areas, the typical Redfield–Brzezinski molar ratios of Si to N (1:1) and N to P (16:1)

are used to represent nutrient stoichiometric requirements for a balanced plankton growth in both freshwater and coastal marine systems (Redfield, 1963; Brzezinski, 1985). For example, the abundance of DSi is an important stimulant for diatoms growth, which helps in transferring energy to higher trophic levels due to higher grazing potential of higher organism such as zooplankton on diatoms (Conley et al., 1993). This implies that non-diatom plankton that may not require DSi for growth may dominate phytoplankton community if DSi is limiting, and this may reduce the trophic importance of diatoms in aquatic systems. Based on laboratory bioassay, DIP may potentially limit primary productivity when the ambient molar ratios of DIN/DIP and DSi/DIP exceeds 22 (Justić et al., 1995). In addition, experimental study by Hu et al. (1990) showed that DIP might be potentially limiting when DIN/ DIP exceeds 30, while DIN limitation would occur when DIN/DIP is <8, for phytoplankton production. Moreover, Kahlert (1998) reported that DIP bio-limitation may occur when DIN/DIP is >32, while DIN biolimitation would occur if DIN/DIP is <12, for phytoplankton production. During this study, the mean molar DIN/DIP ratio was generally higher than the typical Redfield-Brzezinski ratio, and higher than the experimental ratios reported for DIN and DIP limitations in the literature (Hu et al., 1990; Justić et al., 1995; Kahlert, 1998), implying that primary productivity in the MWS is strongly limited by DIP. Although the DSi/DIP ratios obtained in this study were elevated, the DSi/DIN ratios were less than the typical Redfield-Brzezinski ratios, suggesting that DSi may co-limit primary productivity in the MWS. The differences in the nutritional needs of plankton assemblages and biogeochemical processes may have accounted for the spatial variability of nutrient molar ratios as observed in this study (Fig. 4). Based on the assumption that DOP in the MWS is composed of lower molecular weight compounds which could be assimilated by microbial community when DIP is not enough to provide the nutritional needs of living aquatic organisms, the stoichiometric relationship between DIN and (DIP + DOP) was evaluated. Considering the whole dataset, the molar DIN/(DIP + DOP) ratios in this study ranged from ~ 8 to 23 with an average of 12 \pm 4. This showed that DOP is not limiting when scaled to the Redfield-Brzezinski ratio, implying that DOP may be nutritionally important in the MWS because extant microorganism community may simultaneously assimilate DOP as well as DIP. However, changes in molar ratios of the dissolved nutrients in the MWS, especially as DSi and DIP may potentially co-limit primary productivity would affect the proportions and functionality of phytoplankton community (Egge and Aksnes, 1992; Conley et al., 1993). Therefore, the findings in this study suggested that changes in nutrient ratios and dominance of DIN may have important implications on the algal outbreak frequently reported in the MWS in recent

4.2. Relationship between P and physicochemical parameters

The correlations between nutrients and surface water physicochemical parameters such as salinity, pH, and Chl-a, have important implications on the sources and biogeochemical behavior of nutrients including P in coastal waters. Pearson correlation analysis with a two-tail level of significance was conducted on P species, physicochemical parameters and related nutrients contents obtained during this study from the western and eastern flanks of the MWS to have an in-depth understanding of the influencing factors on different P species in the MWS. It is important to note that modifications in nutrient concentrations occur in most coastal marine systems that are influenced by multiple stressors. For instance, significant negative correlation between nutrients and salinity may indicate that saltwater dilution may likely be among the most important factor affecting nutrient concentrations, with the assumption that nutrients in the system of interest are dominantly

derived from riverine source (Dan et al., 2019). Thus, the deviation from such relationships may be attributed to other factors that either add or remove nutrients from surface water. In this study, the result from Pearson correlation analysis showed negative relationship between different P species and salinity, except for DOP (Table 4). The generally decreasing trend of DIP, PIP, POP and TPP from the north to south in the MWS (Fig. 2a-f) and their positive relationship with DIN and DSi (Table 4), indicated that the surface water P is mostly delivered from the adjoining rivers to the MWS. This is consistent with the previous observations in the study area (Yang et al., 2012). On the other hand, P is prone to form insoluble particulate compounds through adsorption, oxidation-reduction, complexation, and co-precipitation with organic matter, metal oxides, and/or ions in aquatic environment (He et al., 2009). A slight increase in PIP contents at the southern region of the eastern flank (station 15) may have resulted from sediment resuspension during tidal mixing. This may be possible, as previous study had reported that sedimentary P in the MWS is dominantly composed of inorganic P (Yang et al., 2019b; Dan et al., 2020a). Although surface water POP can increase via in situ marine primary production (Jensen et al., 1995; Yang et al., 2018b), the gradual increase in surface water POP around the southern region of the eastern flank (site 14) in the MWS may have also resulted from sediment resuspension. In overall, the relationship between TPP with SPM was positive and significant (r =0.52, p < 0.05), while significant negative relationship was observed between TPP and Chl-a (r = -0.57, p < 0.05). These imply that both the SPM and primary productivity played different roles in particulate P dynamics in the MWS.

Generally, DOP dominated the TDP pool in the MWS during this study as discussed earlier (Section 4.1). The pH values (Table 1) in the investigated sites show that alkalinity thrives in surface water of the MWS. Increase in pH causes a shift in phosphate speciation from H₂PO₄ to HPO₄²⁻, and when dissolved P is present in the form of HPO₄²⁻ in alkaline environment, it would be easy for Ca²⁺ and carbonate to produce insoluble P species by co-precipitation (Wang et al., 2012), resulting in lower DIP concentrations as observed in this study. Similar to POP, DOP also generally increased as Chl-a increased along the salinity gradients from the northern to the southern regions at the western and eastern flanks of the MWS. Although somewhat variable, the correlation between Chl-a and DOP was positive and significant (r =0.68; p < 0.01; Table 4), suggesting that DOP is relevant for phytoplankton production in the MWS. DIP showed a significant negative correlation with Chl-a (r = -0.52; p < 0.05; Table 4), which indicated that the reduction in DIP in surface water of the MWS was also partly related to phytoplankton utilization. The average molar DON/DOP ratio during this study was 15.7, which is almost the same as the Redfield N/P ratio of 16:1 required for phytoplankton-balanced growth (Redfield,

Table 4

Pearson correlation matrix for different P species including dissolved inorganic nitrogen and silicate, and physicochemical parameters in surface water of the Maowei Sea (MWS).

	S	pН	DO	Eh	Chl-a	SPM	DIN	DSi	DIP	DOP	TDP	PIP	POP	TPP
S	1													
pН	-0.026	1												
DO	-0.869^{**}	0.077	1											
Eh	0.362	-0.182	-0.622*	1										
Chl-a	0.732^{**}	0.101	-0.727^{**}	0.448	1									
SPM	0.002	0.733**	-0.082	-0.286	-0.015	1								
DIN	-0.442	-0.102	0.512	-0.276	-0.499	-0.082	1							
DSi	-0.700^{**}	0.062	0.607*	-0.363	-0.741^{**}	0.138	0.342	1						
DIP	-0.507	0.296	0.382	-0.341	-0.519*	0.597*	0.431	0.664**	1					
DOP	0.438	0.002	-0.421	0.35	0.685**	-0.252	-0.151	-0.704^{**}	-0.745^{**}	1				
TDP	-0.008	0.384	-0.129	0.075	0.339	0.396	0.331	-0.182	0.19	0.513	1			
PIP	-0.692^{**}	0.42	0.682**	-0.548*	-0.639*	0.484	0.492	0.446	0.731**	-0.502	0.202	1		
POP	-0.518*	0.427	0.34	-0.141	-0.167	0.438	0.047	0.279	0.46	-0.128	0.405	0.525*	1	
TPP	-0.716^{**}	0.468	0.655**	-0.488	-0.570*	0.522*	0.415	0.445	0.730**	-0.446	0.283	0.969**	0.720^{**}	1

^{*} Correlation is significant at the 0.05 level (two-tailed) (n = 15).

^{**} Correlation is significant at the 0.01 level (two-tailed) (n = 15).

1963; Dan et al., 2019). This suggested that the concentrations of DON and DOP are optimal from plankton utilization, and that the sources (i. e., besides anthropogenic input) and distribution of DOP are somewhat influenced by the growth and metabolism of primary producers in surface water of the MWS. Concentration of DOP exceeding that of DIP have been frequently reported in estuarine and coastal surface waters, attributed to phytoplankton production enhancing the DOP released into the seawater (e.g., van Beusekom and de Jonge, 2012; Duan et al., 2016). Therefore, primary productivity by marine plankton plays important role in the concentrations and dynamics of DOP in the MWS.

4.3. Transformation and partitioning of P between dissolved and particulate phases

Various P species can vary significantly in concentrations between dissolved and particulate phases along salinity gradients during mixing processes in aquatic environments, and environmental mixing conditions induces P removal, migration, regeneration and transformation between different species (Lin et al., 2012). Particulate P is important in the cycling of P in coastal waters, and can be transformed into dissolved P by the direct extracellular release from phytoplankton, sloppy feeding by crustacean zooplankton, and cytolysis by viral infection and release of ingested prev organic matter by protozoan grazers or desorption. Although the concentration trend of TPP generally decreased from sites 1-9 at the western flank, our results showed a considerable increase in TDP as TPP declined at salinity range of \sim 3–9 psu around the estuary regions at the western flank (Fig. 2e). Potentially, this indicated that there was desorption and release of P from particulate P phase during estuarine mixing at the western flank. At the eastern flank, it appeared that the reduction in TPP with the corresponding increase in TDP concentrations obviously occurred across the sampling sites where salinity ranged from 1.17-17.96 psu (Fig. 2f). Generally, the sharp decline in TDP in the relatively high salinity of (13–18 psu) and (9–15 psu) sites at the eastern and western flanks, respectively (Fig. 2e-f), suggesting that there was a rapid P removal behavior during later mixing. This may be because fine-grained particles can easily adsorb large amount of TDP by flocculation in saline water environment, which settle to the sediment resulting in the decrease of TDP concentrations (Magni et al., 2002). Therefore, these observations showed that the dynamic transformations of P between dissolved and particulate phase at varying salinity is possible in surface water at the western and eastern flanks of the MWS.

At the western flank, the decrease in the concentration of DIP between the lower salinity (\sim 0.65 psu) site 2 and higher salinity (\sim 9.35 psu) site 8 was 3.33 µM, and comparable to the corresponding increase in DOP (3.26 μM) at these sites. The near balance between DIP and DOP at the lower and higher salinity regions showed that there is a potential transformation of P between DIP and DOP in surface water of the MWS at the western flank. Along the salinity gradients at the eastern flank, the decrease in DIP (1.57 µM) was obviously lower than the corresponding increase in DOP (2.69 µM), but the sum of the reduction in TPP and DIP (i.e., ~2.71 µM) almost balanced the increase in DOP. Therefore, increase in DOP is related to fact that DIP is readily assimilated by aquatic organisms and excreted in the form of DOP, or desorbed and released from particulate P (Lin et al., 2013). For the eastern flank, it may be that zooplankton fed on phytoplankton that utilizes large amount of DIP and then metabolized to insoluble particulate P, which releases lower DIP to surface water as also reported in other study areas (e.g., Benitez-Nelson, 2000; Yoshimura et al., 2018). Previous studies have also shown that DIP can be transformed biologically to DOP through assimilation by marine phytoplankton and/or bacteria (Ruttenberg, 2003). This conclusion can be supported by the significantly negative correlation between DIP and DOP (r = -0.75; p < 0.01) in the MWS (Table 4). In summary, a large-scale migration and/or transformation among P species occurred between the dissolved and particulate phases facilitated by complex biogeochemical processes during estuarine mixing at the western and eastern flanks of the MWS.

Generally, a two-step mechanism for adsorption of DIP by particles is 1) one that proceeds via a fast reaction kinetic step through adsorption or desorption on the particles surface, and 2) through the diffusion of phosphate into the interior of particles that occur in a longer time-scale (Froelich, 1988). Hence, if the kinetic reaction time is slower than the flushing time of an aquatic ecosystem, the chemical reaction processes between dissolved and particulate P phases will not reach equilibrium (Morris, 1990; Fang, 2000). Therefore, the non-equilibrium in the dissolved and particulate P phase may be dependent on the relative timescales of adsorption or desorption processes of different P species due to the continuous inflow of freshwater from the adjoining rivers, irregular diurnal tidal incursion and changes in SPM concentrations induced by sediment resuspension along salinity gradients. This may account for the slightly lower and wider range of P log(K_d) values (Cai et al., 2012) as obtained in the MWS compared to other study areas. Caraco et al. (1990) showed a decrease in P log(K_d) values as salinity increases due to sulphate competition for adsorption sites. Such process promotes desorption at higher salinity. In this study, the P log(K_d) decreased as salinity increases, especially at the eastern flank (Fig. 6a). In addition to some factors discussed in the preceding paragraphs, the decrease in P log (K_d) may be attributed to desorption of P from the particles because of competition from seawater major anions such as Cl⁻ and SO₄ that form soluble chloro and sulfato complexes with metals in solution. A significant negative relationship was also found between the P log(K_d) versus SPM, especially at the eastern flank (Fig. 6b), indicating that P has a strong particle reactivity in the MWS. Moreover, particle concentration effect may have played an important role in regulating the partitioning of inorganic P and TP between dissolved and particulate phases (Li et al., 2017), consistent with the findings in the southwest region of Lake Michigan (Lin and Guo, 2016). In contrast, the weak correlation between the P log(K_d) and SPM at the western flank showed that indeed, several indirect processes affecting P partitioning between the dissolved and particulate phases, are related to biological factors (especially for DOP and POP), while DIP and PIP were mostly influenced by physicochemical factors. In summary, the differences in P $log(K_d)$ values between the MWS and other coastal marine systems (e.g., Lin et al., 2012; Lin and Guo, 2016; Li et al., 2017) may be generally dependent on the levels and spatial distributions of salinity, SPM, pH, aerobic conditions, the texture of particles, adsorbed P, sources of P, flushing time, river flow rate, dissolved organic matter, colloidal P content and alkalinity.

4.4. Effect of rivers discharge on P dynamics

Studies on the influence of riverine discharge on P dynamics are important for understanding the biogeochemical behavior of P. As mentioned in Section 2.1, the annual freshwater discharge from the Maolingjiang River and Qinjiang River into the MWS is 25.9×10^8 m³ y^{-1} and 20.3×10^8 m³ y⁻¹, respectively, and these rivers also co-deliver $\sim \! 8.6 \times 10^4 \text{ tons y}^{-1}$ of suspended sediment load into the MWS (Chen et al., 2018). However, these amount are far less compared to the annual freshwater discharge from other Chinese rivers such the Pearl River (discharge: 3.3×10^{11} m³ y⁻¹, suspended load: 85×10^{7} tons y⁻¹, Li et al., 2017) and Dafengjiang River (discharge: 18.3×10^{9} m³ y⁻¹, suspended load: 11.77×10^4 tons y⁻¹, Yang et al., 2018a). Apparently, more than 80% of these discharges occur during the wet season months (May-September) in the MWS and nearby aquatic systems. Nevertheless, the average TDP (3.84 μM) and TPP (2.14 μM) in the MWS are significantly higher than the amount previously reported in nearby aquatic systems, such as the Dafengjiang River Estuary (TDP \sim 1.05 μ M, TPP \sim 0.19 μ M; Yang et al., 2018a) and Pearl River Estuary (TDP \sim 1.92 μM , TPP $\sim 1.50~\mu M$; Li et al., 2017) during the wet season. The lower concentrations of surface water P in the Pearl River Estuary were reported to be significantly influenced by strong stratification (which had favored the settlement of SPM supplied by freshwater discharge), and thus enhancing more DIP uptake for primary productivity (Li et al., 2017). On the other hand, lower surface water P phases in the Dafengijang River Estuary were attributed to lower P export by the rivers and less anthropogenic P input (Yang et al., 2018a). Moreover, the reduction in surface water P in the Dafengjiang River Estuary surface water also resulted from rapid water exchange between the Dafengjiang River Estuary and the Beibu Gulf. Compared to the nearby aquatic systems with high freshwater discharge rates, it is most likely that differences in dissolved P relative to particulate P in the MWS may result from differences in biogeochemical and physical processes. Among all P species in dissolved and particulate phases, DIP is the most readily bioavailable for primary productivity in surface water, and the continuous freshwater supply, limited water exchange between the MWS and the Beibu Gulf, and primary productivity may have had an important implication on the concentrations and distributions of DIP in the MWS. Thus, we applied a two-end-member mixing model to distinguish the influences of the physical or biological factors on DIP variability in the MWS.

At the western flank, the freshwater and saltwater end-members for surface water salinity and DIP concentrations were 0.63 psu and 1.88 μM and 15.07 psu and 1.33 μM selected from sites 1 and 9, respectively (Tables 1 and 2). At the eastern flank, the freshwater and saltwater endmembers for surface water salinity and DIP concentrations were 1.17 psu and 2.43 µM, and 17.96 psu and 0.91 µM selected from sites 10 and 15, respectively (Tables 1 and 2). As shown in Fig. 6c and the deviation from the theoretical mixing line, positive deviations were found at most of the stations, except for the negative deviation at site 2 for the western flank (Fig. 6d). The positive deviation suggested that DIP variability at the western and eastern flanks of the MWS is also dominantly controlled by biological utilization in addition to absorption/desorption processes. DIP addition was observed near the mouth of the Maolingiang River estuary where industries are clustered (Zhang et al., 2019), which likely contributed to the replenishment of DIP from the perennial industrial sewage discharge. From our data, we found that the reduction in DIP was $1.24\,\mu\text{M}$ and $1.55\,\mu\text{M}$ at the western and eastern flanks, respectively as estimated by the two-end-member model. Thus, it is likely that the bioavailability of DIP for phytoplankton uptake is somewhat higher at the eastern flank (supported by the relatively higher average Chl-a) than at the western flank of the MWS. Therefore, multiple biogeochemical processes control the dynamics of P under the influence of riverine input in surface water of the MWS.

5. Conclusion

This study focused on the P biogeochemistry in dissolved and particulate phases in surface water at the western and eastern flanks of the Maowei Sea (MWS). Total dissolved P (TDP) dominated (TDP/TP = 61.2–70.6%) the total P (TP) pool. Dissolved organic P (DOP) dominated (DOP/TDP = 58.1%–61.1%) the TDP pool. In contrast to dissolved P phase, the total particulate P (TPP) pool was dominated by inorganic P (PIP), which accounted for 68.1-69.1% of TPP. The dominance of TDP pool indicated that the delivery of P from rivers to coastal sea in dissolved phase is as important as particulate phase, especially in less turbid aquatic systems. DIP level in the MWS is lower to medium range compared to other estuarine and coastal systems, while DOP is somewhat elevated in the MWS due to the prevailing intensive mariculture in the MWS, biological production, and/or dissolution from fecal debris and detritus. Increasing anthropogenic sources from the catchment and/ or watershed may also have accounted for the increase in the levels of DIP or DOP (the readily bioavailable P species), which may worsen the frequency of eutrophication depending on how the MWS would respond to external P load. The stoichiometric relationship between DIP, DIN and DSi, suggested that DIP is potentially bio-limiting in the MWS, while DSi may co-limit plankton growth. The dynamic changes, transformation, and distribution of P in dissolved and particulate phases are controlled by physicochemical conditions, freshwater discharge, and biological activities in the MWS. A partitioning coefficient (K_d) approach, which was used to examine the partitioning of P and its particle reactivity

showed that particle concentration effect along the salinity gradients contributed to the partitioning of P between the dissolved and particulate phase. Although subject to some limitations, the two-end-member mixing model suggested that DIP was also influenced by biological factors such as phytoplankton uptake in most of the studied sites. Overall, the study on the dynamic changes in the concentrations, spatial distribution, and transformation process of different P species between dissolved and particulate phases can effectively reveal the biogeochemical behavior of P as well as understanding the internal relationship between the biogeochemical cycling of P and eutrophication.

CRediT authorship contribution statement

Cheng Xu: Writing - original draft, Writing - review & editing. Solomon Felix Dan: Writing - review & editing. Bin Yang: Methodology, Writing - review & editing. Dongliang Lu: Investigation. Zhenjun Kang: Investigation. Haifang Huang: Investigation. Jiaodi Zhou: Data curation. Zhiming Ning: Formal analysis.

Declaration of Competing Interest

The authors declare that they have no known competing financial interests or personal relationships that could have appeared to influence the work reported in this paper.

Acknowledgement

We sincerely thank our colleagues from the marine biogeochemistry laboratory for their help in field sampling. This work was supported by grants from the National Natural Science Foundation of China (Nos. 41706083 and 41966002), the Guangxi Natural Science Foundation, China (Nos. 2018GXNSFDA281025 and 2018GXNSFAA281295), the Opening Project of Guangxi Laboratory on the Study of Coral Reefs in the South China Sea (No. GXLSCRSCS2018002), the Guangxi "Marine Ecological Environment" Academician Workstation Capacity Building (No. Gui Science AD17129046) and the Distinguished Experts Programme of Guangxi Province.

Appendix A. Supplementary data

Supplementary data to this article can be found online at https://doi.org/10.1016/j.jhydrol.2020.125822.

References

- Abdel-Satar, A.M., Ali, M.H., Goher, M.E., 2017. Indices of water quality and metal pollution of Nile River, Egypt. Egyptian. J. Aquat. Res. 43, 21–29.
- Alvarez-Vazquez, M.A., Prego, R., Ospina-Alvarez, N., Caetano, M., Patricia Bernardez, P., Doval, M., Filgueiras, A.V., Vale, C., 2016. Anthropogenic changes in the fluxes to estuaries: wastewater discharges compared with river loads in small rias. Estuar. Coast. Shelf Sci. 179, 112–123.
- Aspila, K.I., Agemian, H., Chau, A.S.Y., 1976. A semi-automated method for the determination of inorganic, organic and total phosphate in sediments. Analyst 101, 187–197.
- Ayers, J.C., Watson, E.B., 1991. Solubility of apatite, monazite, zircon, and rutile in supercritical aqueous fluids with implications for subduction zone geochemistry. Philos. Trans. R. Soc. Lond. A 335, 365–375.
- Benitez-Nelson, C.R., 2000. The biogeochemical cycling of phosphorus in marine systems. Earth-Sci. Rev. 51, 109–135.
- Björkman, K.M., Karl, D.M., 2003. Bioavailability of dissolved organic phosphorus in the euphotic zone at Station ALOHA, North Pacific Subtropical Gyre. Limnol. Oceanogr. 48, 1049–1057.
- Brzezinski, M.A., 1985. The Si/C/N ratio of marine diatoms: interspecific variability and the effect of some environmental variables. J. Phycol. 21, 347–357.
- Cai, Y., Guo, L., 2009. Abundance and variation of colloidal organic phosphorus in riverine, estuarine, and coastal waters in the northern Gulf of Mexico. Limnol. Oceanogr. 54, 1393–1402.
- Cai, Y., Guo, L., Douglas, T.A., Whitledge, T.E., 2008. Seasonal variations in nutrient concentrations and speciation in the Chena River, Alaska. J. Geophys. Res. 113, G03035. https://doi.org/10.1029/2008JG000733.

- Cai, Y., Guo, L., Wang, X., Mojzis, A.K., Redalje, D.G., 2012. The source and distribution of dissolved and particulate organic matter in the Bay of St. Louis, northern Gulf of Mexico. Estuar. Coast. Shelf Sci. 96, 96–104.
- Caraco, N., Cole, J., Likens, G.E., 1990. A comparison of phosphorus immobilization in sediments of freshwater and coastal marine systems. Biogeochemistry 9, 277–290.
- Chen, X., Lao, Y., Wang, J., Du, J., Liang, M., Yang, B., 2018. Submarine groundwaterborne nutrients in a tropical bay (Maowei Sea, China) and their impacts on the oyster aquaculture. Geochem. Geophys. Geosyst. 19, 932–951.
- Conley, D.J., Schelske, C.L., Eugene, F.S., 1993. Modification of the biogeochemical cycle of silica with eutrophication. Mar. Ecol. Prog. Ser. 101, 171–192.
- Cozzi, S., Ibánez, C., Lazar, L., Raimbault, P., Giani, M., 2019. Flow regime and nutrient-loading trends from the largest south European watersheds: implications for the productivity of Mediterranean and Black Sea's coastal areas. Water 11. https://doi.org/10.3390/w11010001.
- Dan, S.F., Lan, W., Yang, B., Han, L., Xu, C., Lu, D., Kang, Z., Huang, H., Ning, Z., 2020a. Bulk sedimentary phosphorus in relation to organic carbon, sediment textural properties and hydrodynamics in the northern Beibu Gulf, South China Sea. Mar. Pollut. Bull. 155, 111176.
- Dan, S.F., Liu, S.M., Udoh, E.C., Ding, S., 2019. Nutrient biogeochemistry in the Cross River estuary system and adjacent Gulf of Guinea, South East Nigeria (West Africa). Cont. Shelf Res. 179, 1–17.
- Dan, S.F., Liu, S.M., Yang, B., 2020b. Geochemical fractionation, potential bioavailability and ecological risk of phosphorus in surface sediments of the Cross River estuary system and adjacent shelf, south East Nigeria (West Africa). J. Mar. Syst. 201, 103244
- Diaz, J.M., Björkman, K.M., Haley, S.T., Ingall, E.D., Karl, D.M., Longo, A.F., Dyhrman, S. T., 2016. Polyphosphate dynamics at Station ALOHA, North Pacific subtropical gyre. Limnol. Oceanogr. 61, 227–239.
- Duan, L.Q., Song, J.M., Yuan, H.M., Li, X.G., Li, N., 2016. Distribution, partitioning and sources of dissolved and particulate nitrogen and phosphorus in the north Yellow Sea. Estuar. Coast Shelf Sci. 181, 182–195.
- Duan, S., Liang, T., Zhang, S., Wang, L., Zhang, X., Chen, X., 2008. Seasonal changes in nitrogen and phosphorus transport in the lower Changjiang River before the construction of the Three Gorges Dam. Estuar. Coast. Shelf Sci. 79, 239–250.
- Egge, J.K., Aksnes, D.L., 1992. Silicate as regulating nutrient in phytoplankton competition. Mar. Ecol. Prog. Ser. 83, 281–289.
- Eliani-Russak, E., Herut, B., Orit Sivan, O., 2013. The role of highly stratified nutrientrich small estuaries as a source of dissolved inorganic nitrogen to coastal seawater, the Qishon (SE Mediterranean) case. Mar. Pollut. Bull. 71, 250–258.
- Fang, T.H., Wang, C.W., 2020. Dissolved and particulate phosphorus species partitioning and distribution in the Danshuei River Estuary, Northern Taiwan. Mar. Pollut. Bull 151, 110839.
- Fang, T.H., 2000. Partitioning and behaviour of different forms of phosphorus in the Tanshui Estuary and one of its tributaries, Northern Taiwan. Estuar. Coast. Shelf Sci. 50, 689–701.
- Froelich, P.N., 1988. Kinetic control of dissolved phosphate in natural rivers and estuaries: a primer on the phosphate buffer mechanism 1. Limnol. Oceanogr. 33, 649–668
- Gu, Y.G., Huang, H.H., Liu, Y., Gong, X.Y., Liao, X.L., 2018. Non-metric multidimensional scaling and human risks of heavy metal concentrations in wild marine organisms from the Maowei Sea, the Beibu Gulf, South China Sea. Environ. Toxicol. Phar. 59, 119–124.
- Gu, Y.G., Lin, Q., Yu, Z.L., Wang, X.N., Ke, C.L., Ning, J.J., 2015. Speciation and risk of heavy metals in sediments and human health implications of heavy metals in edible nekton in Beibu Gulf, China: A case study of Qinzhou Bay. Mar. Pollut. Bull. 101, 852–859.
- Hansen, H. P., Koroleff, F., 1999. Determination of nutrients. In Grasshoff, K., Kremling, K., Ehrhardt, M., (Eds.), Methods of Seawater Analysis, WILEY-VCH, Weinheim, Germany, pp. 159–288, ISBN 3-527-29589-5.
- He, H., Chen, H., Yao, Q., Qin, Y., Mi, T., Yu, Z., 2009. Behavior of different phosphorus species in suspended particulate matter in the Changjiang estuary. Chin. J. Oceanol. Limn. 27, 859–868.
- Ho, A.Y., Xu, J., Yin, K., Jiang, Y., Yuan, X., He, L., Harrison, P.J., 2010. Phytoplankton biomass and production in subtropical Hong Kong waters: influence of the Pearl River outflow. Estuar. Coast. 33, 170–181.
- House, W.A., 2003. Geochemical cycling of phosphorus in rivers. Appl. Geochem. 18, 739–748.
- Hu, M., Yang, Y., Xu, C., Harrison, P.J., 1990. Phosphate limitation of phytoplankton growth in the Changjiang Estuary. Acta Oceanol. Sin. En. Ed. 9, 405–411.
- Jensen, H.S., Bendixen, T., Andersen, F.Ø., 2006. Transformation of particle-bound phosphorus at the land-sea interface in a Danish estuary. Wat. Air. Soil poll. Focus 6, 547–555.
- Jensen, H.S., Mortensen, P.B., Andersen, F.O., Jensen, A., 1995. Phosphorus cycling in a coastal marine sediment, Aarhus Bay, Denmark. Limnol. Oceanogr. 36, 908–917.
- Jordan, T.E., Cornwell, J.C., Boynton, W.R., Anderson, J.T., 2008. Changes in phosphorus biogeochemistry along an estuarine salinity gradient: The iron conveyer belt. Limnol. Oceanogr. 53 (1), 172–184.
- Justić, D., Rabalais, N.N., Turner, R.E., Dortch, Q., 1995. Changes in nutrient structure of river-dominated coastal waters: stoichiometric nutrient balance and its consequences. Estuar. Coast. Shelf Sci. 40, 339–356.
- Kahlert, M., 1998. C/N/P: ratios of freshwater benthic algae. Arch. Hydrobiol. Spec. Issue Adv. Limnol. 51, 105–114.
- Karl, D.M., 2014. Microbially mediated transformations of phosphorus in the sea: new views of an old cycle. Annu. Rev. Mar. Sci. 6, 279–337.
- Lemley, D.A., Adams, J.B., Taljaard, S., Strydom, N.A., 2015. Towards the classification of eutrophic condition in estuaries. Estuar. Coast. Shelf Sci. 164, 221–232.

- Li, R., Xu, J., Li, X., Shi, Z., Harrison, P.J., 2017. Spatiotemporal variability in phosphorus species in the Pearl River Estuary: influence of the river discharge. Sci. Rep. 7, 13649.
- Lin, P., Chen, M., Guo, L., 2012. Speciation and transformation of phosphorus and its mixing behavior in the Bay of St. Louis estuary in the northern Gulf of Mexico. Geochim. Cosmochim. Acta 87, 283–298.
- Lin, P., Guo, L., 2016. Dynamic changes in the abundance and chemical speciation of dissolved and particulate phosphorus across the river-lake interface in southwest Lake Michigan. Limnol. Oceanogr. 61, 771–789.
- Lin, P., Guo, L., Chen, M., Cai, Y., 2013. Distribution, partitioning and mixing behavior of phosphorus species in the Jiulong River estuary. Mar. Chem. 157, 93–105.
- Lin, P., Klump, J.V., Guo, L., 2016. Dynamics of dissolved and particulate phosphorus influenced by seasonal hypoxia in Green Bay, Lake Michigan. Sci. Total Environ. 541, 1070–1082.
- Lin, P., Klump, J.V., Guo, L., 2018. Variations in chemical speciation and reactivity of phosphorus between suspended-particles and surface-sediment in seasonal hypoxiainfluenced Green Bay. J. Great Lakes Res. 44, 864–874.
- Liu, H., Chen, M., Shen, P., Huang, H., Dai, M., Qi, Z., 2016. A first description of ciliate assemblages in a subtropical, eutrophic bay, South China Sea: species assemblage and environmental correlates-Ciliate variation in a subtropical bay. Aquat. Living Resour. 29, 304.
- Liu, S.M., Hong, G.H., Zhang, J., Ye, X.W., Jiang, X.L., 2009. Nutrient budgets for large Chinese estuaries. Biogeosciences 6, 2245–2263.
- Liu, S.M., Zhang, J., Chen, H.T., Zhang, G.S., 2005. Factors influencing nutrient dynamics in the eutrophic Jiaozhou Bay, North China. Prog. Oceanogr. 66, 66–85.
- Liu, S.M., Zhang, J., Li, D.J., 2004. Phosphorus cycling in sediments of the Bohai and Yellow Seas. Estuar. Coast. Shelf Sci. 59, 209–218.
- Lu, F.H., Ni, H.G., Liu, F., Zeng, E.Y., 2009. Occurrence of nutrients in riverine runoff of the Pearl River Delta, South China. J. Hydrol. 376, 107–115.
- Mackenzie, F.T., Ver, L.M., Lerman, A., 2002. Century-scale nitrogen and phosphorus controls of the carbon cycle. Chem. Geol. 190, 13–32.
- Magni, P., Montani, S., Tada, K., 2002. Semidiurnal dynamics of salinity, nutrients and suspended particulate matter in an estuary in the Seto Inland Sea, Japan, during a spring tide cycle. J. Oceanogr. 58, 389–402.
- Meng, X., Xia, P., Li, Z., Meng, D., 2016. Mangrove degradation and response to anthropogenic disturbance in the Maowei Sea (SW China) since 1926 AD: Mangrovederived OM and pollen. Org. Geochem. 98, 166–175.
- derived OM and pollen. Org. Geochem. 98, 166–175.

 MOAC (Ministry of Agriculture, China), 2017. China Fisheries Yearbook, 2016. China Agriculture Publisher, Beijing, China.
- Morris, A.W., 1990. Kinetic and equilibrium approaches to estuarine chemistry. Sci. Total Environ. 97, 253–266.
- Pan, F., Guo, Z.R., Cai, Y., Fu, Y.Y., Wu, J.Y., Wang, B., Liu, H.T., Gao, A.G., 2020. Cyclical patterns and (im)mobilization mechanisms of phosphorus in sediments from a small creek estuary: evidence from in situ monthly sampling and indoor experiments. Water Res. 171, 115479.
- Pan, K., Wang, W.X., 2012. Trace metal contamination in estuarine and coastal environments in China. Sci. Total Environ. 421 (422), 3–16.
- Parsons, T.R., Maita, Y., Lalli, C.M., 1984. A manual of chemical and biological methods for seawater analysis. Pergamon, Oxford sized algae and natural seston size fractions. Mar. Ecol. Prog. Ser. 199, 43–53.
- Paytan, A., McLaughlin, K., 2007. The oceanic phosphorus cycle. Chem. Rev. 107, 563–576.
- Piper, M.M., Benitez-Nelson, C.R., Frey, K.E., Mills, M.M., Pal, S., 2016. Dissolved and particulate phosphorus distributions and elemental stoichiometry throughout the Chukchi Sea. Deep-Sea Res. Pt. II. 130, 76–87.
- Prastka, K.E., Malcolm, S.J., 1994. Particulate phosphorus in the Humber estuary. Netherland J. Aquat. Ecol. 28, 397–403.
- Prastka, K., Sanders, R., Jickells, T., 1998. Has the role of estuaries as sources or sinks of dissolved inorganic phosphorus changed over time? Results of a K_d study. Mar. Pullut. Bull. 36, 718–728.
- Redfield, A.C., 1963. The influence of organisms on the composition of seawater. The Sea $2,\,26$ –77.
- Ruttenberg, K.C., 2003. The global phosphorus cycle. Treat. Geochem. 8, 682.
- Shim, M.J., Swarzenski, P.W., Shiller, A.M., 2012. Dissolved and colloidal trace elements in the Mississippi River delta outflow after Hurricanes Katrina and Rita. Cont. Shelf Res. 42, 1–9.
- Shinohara, R., Ouellette, L., Nowell, P., Parsons, C.T., Shin-ichiro, S.M., Voroney, R.P., 2018. The composition of particulate phosphorus: A case study of the Grand River, Canada. J. Great Lakes Res. 44, 527–534.
- Slomp, C.P., Thomson, J., de Lange, G.J., 2004. Controls on phosphorus regeneration and burial during formation of eastern Mediterranean sapropels. Mar. Geol. 203, 141–159.
- Solórzano, L., Sharp, J.H., 1980. Determination of total dissolved phosphorus and particulate phosphorus in natural waters1. Limnol. Oceanogr. 25, 754-758.
- Tian, H.T., Hu, X.S., Zhang, S.F., Xie, J., Zhang, D., An, J.S., 2014. Distribution and potential ecological risk assessment of heavy metals insurface sediments of Maowei Sea. Mar. Environ. Sci. 33, 187–191 (in Chinese).
- Turner, A., 1996. Trace-metal partitioning in estuaries: importance of salinity and particle concentration. Mar. Chem. 54, 27–39.
- van Beusekom, J.E.E., de Jonge, V.N., 2012. Dissolved organic phosphorus: an indicator of organic matter turnover? Estuar. Coast. Shelf Sci. 108, 29–36.
- van der Zee, C., Roevros, N., Chou, L., 2007. Phosphorus speciation, transformation and retention in the Scheldt estuary (Belgium/The Netherlands) from the freshwater tidal limits to the North Sea. Mar. Chem. 106, 76–91.

- Vilmin, L., Aissa-Grouz, N., Garnier, J., Billen, G., Mouchel, J.M., Poulin, M., Flipo, N., 2015. Impact of hydro-sedimentary processes on the dynamics of soluble reactive phosphorus in the Seine River. Biogeochemistry 122, 229–251.
- Wang, J.J., Beusen, A.H.W., Liu, X.C., Bouwman, A.F., 2020a. Aquaculture production is a large, spatially concentrated source of nutrients in Chinese freshwater and coastal seas. Environ. Sci. Technol. 54, 1464–1474.
- Wang, B., Xin, M., Wei, Q., Xie, L., 2018. A historical overview of coastal eutrophication in the China Seas. Mar. Pollut. Bull. 136, 394–400.
- Wang, F.F., Qu, J.H., Hu, Y.S., 2012. Spatio-temporal characteristics and correlation of phosphate, pH and alkaline phosphatase on water-sediment interface of Lake Taihu. Ecol. Environ. Sci. 21, 907–912 (in Chinese).
- Wang, Q., Li, H., Zhang, Y., Wang, X., Xiao, K., Zhang, X., Dan, S.F., 2020b. Submarine groundwater discharge and its implication for nutrient budgets in the western Bohai Bay, China. J. Environ. Radioact. 212, 106132.
- Wang, Y.J., Liao, R.Q., Liu, W.L., Kannan, K., Ohura, T., Wu, M.H., Ma, J., 2017. Chlorinated polycyclic aromatic hydrocarbons in surface sediment from Maowei Sea, Guangxi, China: occurrence, distribution, and source apportionment. Environ. Sci. Pollut. R. 24, 16241–16252.
- Wei, C.X., Zhao, S., Song, L.R., Wu, H.P., 2017. Analysis and assessment of nutrient status in Maowei Sea of inner Qinzhou Bay. Environ. Sci. Manage. 42, 148–153 (in Chinese)
- Xu, C., Yang, B., Dan, S.F., Zhang, D., Liao, R., Lu, D., Li, R., Ning, Z., Peng, S., 2020. Spatiotemporal variations of biogenic elements and sources of sedimentary organic matter in the largest oyster mariculture bay (Maowei Sea), Southwest China. Sci. Total Environ. 730, 139056.
- Yan, X., Zhai, W., Hong, H., Guo, W., Huang, X., 2012. Distribution, fluxes and decadal changes of nutrients in the Jiulong River Estuary, Southwest Taiwan Strait. Chin. Sci. Bull. 57, 2307–2318.
- Yang, B., Fang, H.Y., Zhong, Q.P., Zhang, C.X., Li, S.P., 2012. Distribution characteristics of nutrients and eutrophication assessment in summer in Qinzhou Bay. Mar. Sci. Bull. 31, 640–645 (in Chinese).
- Yang, B., Kang, Z.J., Lu, D.L., Dan, S.F., Ning, Z.M., Lan, W.L., Zhong, Q.P., 2018a. Spatial variations in the abundance and chemical speciation of phosphorus across the river–sea interface in the northern Beibu Gulf. Water 10, 1103.

- Yang, B., Lan, R.Z., Lu, D.L., Dan, S.F., Kang, Z.J., Jiang, Q.C., Lan, W.L., Zhong, Q.P., 2019a. Phosphorus biogeochemical cycling in intertidal surface sediments from the Maowei Sea in the northern Beibu Gulf. Reg. Stud. Mar. Sci. 28, 100624.
- Yang, B., Liu, S.M., Wu, Y., Zhang, J., 2016. Phosphorus speciation and availability in sediments off the eastern coast of Hainan Island, South China Sea. Cont. Shelf Res. 118, 111–127.
- Yang, B., Liu, S.M., Zhang, G.L., 2018b. Geochemical characteristics of phosphorus in surface sediments from the continental shelf region of the northern South China Sea. Mar. Chem. 198, 44–55.
- Yang, B., Zhou, J.B., Lu, D.L., Dan, S.F., Zhang, D., Lan, W.L., Cui, D.Y., 2019b. Phosphorus chemical speciation and seasonal variations in surface sediments of the Maowei Sea, northern Beibu Gulf. Mar. Pollut. Bull. 141, 61–69.
- Yoshimura, T., Nishioka, J., Ogawa, H., Kuma, K., Saito, H., Tsuda, A., 2014. Dissolved organic phosphorus production and decomposition during open ocean diatom blooms in the subarctic Pacific. Mar. Chem. 165, 46–54.
- Yoshimura, T., Nishioka, J., Ogawa, H., Tsuda, A., 2018. Dynamics of particulate and dissolved organic and inorganic phosphorus during the peak and declining phase of an iron-induced phytoplankton bloom in the eastern subarctic Pacific. J. Mar. Syst. 177 1–7
- Yuan, H., Song, J., Xing, J., Li, X., Li, N., Duan, L., Wang, Q., 2018. Spatial and seasonal variations, partitioning and fluxes of dissolved and particulate nutrients in Jiaozhou Bay. Cont. Shelf Res. 171, 140–149.
- Zhang, D., Lu, D., Yang, B., Zhang, J., Ning, Z., Yu, K., 2019. Influence of natural and anthropogenic factors on spatial-temporal hydrochemistry and the susceptibility to nutrient enrichment in a subtropical estuary. Mar. Pollut. Bull. 146, 945–954.
- Zhang, J.Z., Guo, L., Fischer, C., 2010. Abundance and chemical speciation of phosphorus in sediments of the Mackenzie River Delta, the Chukchi Sea and the Bering Sea: importance of detrital apatite. Aquat. Geochem. 16, 353–371.
- Zhang, Y., Bleeker, A., Liu, J., 2015. Nutrient discharge from China's aquaculture industry and associated environmental impacts. Environ. Res. Lett. 10, 045002.
- Zhang, Y., Gao, X., Wang, C., Chen, C.T.A., Zhou, F., Yang, Y., 2016. Geochemistry of P in sediment cores from Sishili Bay. China. Mar. Pollut. Bull. 113, 552–558.
- Zhou, F.X., Gao, X.L., Yuan, H.M., Song, J.M., Chen, C.T.A., Lui, H.K., Zhang, Y., 2016. Geochemical forms and seasonal variations of phosphorus in surface sediments of the East China Sea shelf. J. Mar. Syst. 159, 41–54.